Scalable Predictive Control and Optimization for Grid Integration of Large-Scale Distributed Energy Resources

Preprint

Abinet Tesfaye Eseye, Bernard Knueven, Deepthi Vaidhynathan and Jennifer King

National Renewable Energy Laboratory

Presented at the 2022 IEEE Power & Energy Society General Meeting
Denver, Colorado
July 17-21, 2022

NREL is a national laboratory of the U.S. Department of Energy
Office of Energy Efficiency & Renewable Energy
Operated by the Alliance for Sustainable Energy, LLC

This report is available at no cost from the National Renewable Energy Laboratory (NREL) at www.nrel.gov/publications.

Contract No. DE-AC36-08GO28308

Conference Paper
NREL/CP-2C00-81506
February 2022

Scalable Predictive Control and Optimization for Grid Integration of Large-Scale Distributed Energy Resources

Preprint

Abinet Tesfaye Eseye, Bernard Knueven, Deepthi Vaidhynathan and Jennifer King

National Renewable Energy Laboratory

Suggested Citation
Eseye, Abinet Tesfaye, Bernard Knueven, Deepthi Vaidhynathan and Jennifer King. 2022. *Scalable Predictive Control and Optimization for Grid Integration of Large-Scale Distributed Energy Resources: Preprint*. Golden, CO: National Renewable Energy Laboratory. NREL/CP-2C00-81506. https://www.nrel.gov/docs/fy22osti/81506.pdf.

NREL is a national laboratory of the U.S. Department of Energy
Office of Energy Efficiency & Renewable Energy
Operated by the Alliance for Sustainable Energy, LLC

This report is available at no cost from the National Renewable Energy Laboratory (NREL) at www.nrel.gov/publications.

Contract No. DE-AC36-08GO28308

Conference Paper
NREL/CP-2C00-81506
February 2022

National Renewable Energy Laboratory
15013 Denver West Parkway
Golden, CO 80401
303-275-3000 • www.nrel.gov

Scalable Predictive Control and Optimization for Grid Integration of Large-scale Distributed Energy Resources

Abinet Tesfaye Eseye, Bernard Knueven, Deepthi Vaidhynathan and Jennifer King
National Renewable Energy Laboratory (NREL)
Golden, Colorado, USA 80401
AbinetTesfaye.Eseye, Bernard.Knueven, Deepthi.Vaidhynathan, Jennifer.King@nrel.gov

***Abstract*— Integrating a large number of distributed energy resources (DERs) into the power grid needs a scalable power balancing method. We formulate the power balancing problem as a look-ahead optimization problem to be solved sequentially by a power distribution system aggregator based on a model predictive control (MPC) framework. Solving large-scale look-ahead control problems requires proper configuration of the control steps. In this paper, to solve large-scale control problems, we propose a variable time granularity where control time steps nearby the current control step have finer resolutions. The aggregator objective includes maximization of power production revenue and minimization of power purchasing expense, renewable power curtailment, and mileage costs for energy storage and electric vehicle (EV) charging stations while satisfying system capacity and operational constraints. The control problem is formulated as a mixed-integer linear program (MILP) and solved using the XpressMP solver. We perform simulations considering a copper plate representation of a large distribution network consisting of 2507 devices (controllable DERs), including curtailable photovoltaics (PVs), energy storage batteries, EV charging stations, and buildings with heating, ventilation, and air conditioning units (HVACs). We show the effectiveness of the proposed approach in managing DERs interactively for maximum energy trading profit and local supply-demand power balancing. Finally, we demonstrate that the proposed method outperforms other benchmark controllers regarding computation time without compromising operational performance.**

***Index Terms*— Distribution system, DER, grid integration, electricity market, model predictive control, power balancing.**

I. INTRODUCTION

A large number of distributed energy resources (DERs) with controllable power set-points are expected to be part of the future power grid [1]. Examples of these DERs are photovoltaics (PVs), energy storage systems (ESSs), electric vehicles (EVs), and buildings with heating, ventilation, and air conditioning units (HVACs). If integrated together in a large-scale system, these DERs could potentially offer flexibility to the larger transmission system and its associated market. In addition, if the DERs are controlled and coordinated well, they can help to balance the fluctuating power generation instigated by renewable energy resources such as wind and solar. In day-ahead electricity markets, DERs can help to maximize the revenue of an aggregator operating and managing them. In real-time power markets, DERs can help to reduce power imbalances caused by forecast errors and provide ancillary services, such as regulation reserve. Finally, by effectively shaving peak power demand, the integration of large numbers of DERs can forestall the need for expensive bulk electric system upgrades like additional generation, storage, or transmission capacity.

Controlling a large number of DERs with inter-temporal constraints (such as ESSs, EVs, and buildings) and periodic variations (such as PVs) requires look-ahead formulations with fast evaluation of the control algorithm that coordinates the DERs and market signals (price, economic dispatch, or automatic generation control signal). Therefore, efficient and reasonably fast methods for solving this large-scale look-ahead control problem in real time are of upmost importance.

The state-of-the-art and recent studies on control and optimization for grid integration of DERs are presented next. The study in [2] proposed distributed feedback controllers that instantaneously regulate DER inverter power outputs. An online algorithm for aggregations of DERs in distribution grids to offer regulation services in response to up-stream transmission grid requests is introduced in [3]. The work in [4] presented a scalable hierarchical algorithm to solve optimal power flow (OPF) problems in a distribution system that targets to dispatch DERs for voltage control at a reduced cost. However, although these studies demonstrated success for optimal control of integrating large numbers of DERs in large-scale distribution grids, they are only applicable for single-step control problems and do not have look-ahead control capability over certain future operating periods. The works in [5]-[8] proposed look-ahead controllers to optimally manage DERs in distribution systems for different control horizons and objectives. However, these works considered a limited number of DERs in the range of a few tens and their scalability to massive DERs, in the range of thousands to millions, is not presented or guaranteed.

In this paper, we formulate the large-scale and look-ahead

This work was authored by the National Renewable Energy Laboratory (NREL), operated by Alliance for Sustainable Energy, LLC, for the U.S. Department of Energy (DOE) under Contract No. DE-AC36-08GO28308. Funding provided by the NREL Laboratory Directed Research and Development (LDRD) program. The views expressed in the article do not necessarily represent the views of the DOE or the U.S. Government.

This research was performed using computational resources sponsored by DOE's Office of Energy Efficiency and Renewable Energy located at NREL.

power balancing and trading problem through the control of massive DERs based on forecasted information of distribution system load demand, renewable power production and power price. We formulate the control problem as a multi-period and variable-time granularity optimization problem, which is solved sequentially by a distribution system aggregator in a model predictive control (MPC) framework.

The novel contributions of this paper include: (1) look-ahead optimization formulation for the control of a massive number of devices (DERs) in distribution systems; (2) multi-time scale (variable time granularity) formulation of the optimal control problem to enhance scalability; and (3) a computational demonstration against two alternative MPC formulations not utilizing variable time granularity.

The remaining sections of the paper are organized as follows. The proposed control approach and problem formulation are presented in Section II. Section III provides the case studies and simulation results. The paper conclusion and future works are given in Section IV.

II. PROPOSED CONTROL APPROACH AND PROBLEM FORMULATION

We consider a large-scale distribution system containing thousands of electrical nodes and controllable devices (DERs). To solve the large-scale look-ahead control problem, we propose a variable time granularity where control time steps nearby the current control step have finer resolutions (5 min) and then the control resolution increases to 10 min, 15 min, 30 min, 1 h, and 2 h as the control time involves over the control horizon, as shown in Fig. 1.

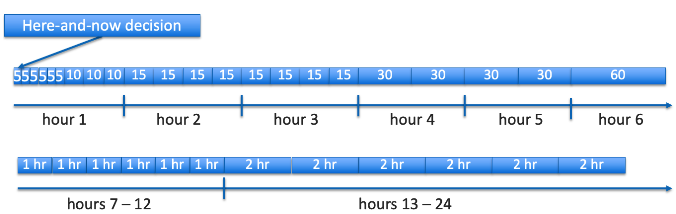

Fig. 1. Variable granularity implementation of the proposed look-ahead control approach.

As shown in Fig. 1, the proposed implementation uses a 24-hour look-ahead window with 34 unequal-length discretized time periods. The approach is easily configured for longer/shorter durations and different time discretizations. The MPC only uses the decision in the first time-step and re-optimizes the system operation every 5 minutes. The objective function and constraints of the proposed look-ahead control approach are presented in the following subsections.

A. Objective Function

The distribution feeder aggregator objective function is given in (1), and it includes net power production revenue, solar power curtailment penalty, and mileage costs of energy storage batteries and EVs.

$$f = f_1 + f_2 + f_3 + f_4 \tag{1}$$

where f_1, f_2, f_3, and f_4 are functions associated with the distribution system aggregator power trading expense or revenue, solar power curtailment penalty, energy storage battery mileage (degradation) cost and electric vehicle supply equipment (EVSE) (or charging station) operation and maintenance (O&M) cost, respectively, and they are defined as follows.

$$f_1 = \sum_{t \varepsilon T} e_t P_t^{fh} \Delta t \tag{2}$$

$$f_2 = \sum_{i \varepsilon N} \sum_{t \varepsilon T} \alpha_t P_{i,t}^{pv,curt} \Delta t \tag{3}$$

$$f_3 = \sum_{i \varepsilon N} \sum_{t \varepsilon T} (\delta_t P_{i,t}^{es,c} + \gamma_t P_{i,t}^{es,d}) \Delta t \tag{4}$$

$$f_4 = \sum_{i \varepsilon N} \sum_{t \varepsilon T} \mu_t P_{i,t}^{evse} \Delta t \tag{5}$$

where e_t is the electricity locational marginal price (LMP) at the feeder head (sub-station bus), α_t is the penalty for solar power curtailments, δ_t and γ_t are mileage costs for charging and discharging the energy storage devices, respectively, μ_t is the O&M cost of EVSEs, Δt is the duration of control step t, T is the control horizon, i is the node/device index, and N is the number of nodes/devices. P_t^{fh} is the feeder head power that the distribution system aggregator trades with the electricity market, P_t^{fh} is positive if the aggregator buys power from the market and negative if the aggregator sells power to the market. $P_{i,t}^{pv,curt}$ is the solar power curtailment, $P_{i,t}^{es,c}$ and $P_{i,t}^{es,d}$ are the charging and discharging power of the energy storage devices, respectively, and $P_{i,t}^{evse}$ is the aggregate charging power of the EVSEs.

The optimal control problem, in this paper, is therefore a minimization of the objective function f expressed in (1) and is given in standard form below.

$$\min_{DV} f \tag{6}$$

where $DV = \{P_t^{fh}, P_{i,t}^{pv,curt}, P_{i,t}^{es}, a_{i,t}^{es}, b_{i,t}^{es}, SOC_{i,t}^{es}, P_{i,t}^{evse}, E_{i,t}^{evse}, P_{i,t}^{hvac}, c_{i,t}^{hvac}, d_{i,t}^{hvac}, T_{i,t}^{bldg}\}$ is the set of decision variables, of the optimal control problem, that need to be determined. $P_{i,t}^{es}$ is the net (charging and discharging) power of the energy storage systems; $a_{i,t}^{es}$ and $b_{i,t}^{es}$ are binary variables indicating the charging and discharging status of the energy storage systems, respectively; $SOC_{i,t}^{es}$ is the state of charge (SOC) of the energy storage devices; $E_{i,t}^{evse}$ is the aggregate energy demanded by EVs at EVSEs; $P_{i,t}^{hvac}$ is the net (heating and cooling) power of the HVACs; $c_{i,t}^{hvac}$ and $d_{i,t}^{hvac}$ are binary variables indicating the heating and cooling status of the HVAC units, respectively; and $T_{i,t}^{bldg}$ is the indoor temperature of buildings.

B. Constraints

The objective function in (6) is subjected to a number of capacity and operational constraints such as feasible power ranges of the DERs, curtailment limits of renewables, SOC limits and dynamics of energy storage systems, power demand and energy dynamics of EVSEs, building thermal dynamics and temperature comforts, and power supply-demand balance. The formulation of these constraints is presented next for each device.

1) *PV Power Generator*

The PV power constraint includes the power curtailment feasible range given below [9].

$$0 \leq P_{i,t}^{pv,curt} \leq P_{i,t}^{pv} \tag{7}$$

where $P_{i,t}^{pv}$ is the solar power forecast at PV i and time t.

2) *Energy Storage System*

The storage constraints include the charging/discharging power feasible range, charging/discharging complementary, net power constraints, SOC bounds, and dynamics [7]. They are defined as follows:

$$\begin{aligned} 0 \leq P_{i,t}^{es,c} &\leq a_{i,t} P_i^{es,max} \\ 0 \leq P_{i,t}^{es,d} &\leq b_{i,t} P_i^{es,max} \\ a_{i,t} + b_{i,t} &\leq 1 \\ P_{i,t}^{es} = P_{i,t}^{es,d} &- P_{i,t}^{es,c} \end{aligned} \tag{8}$$

$$SOC_{i,min}^{es} \leq SOC_{i,t}^{es} \leq SOC_{i,max}^{es} \tag{9}$$

$$SOC_{i,t}^{es} = SOC_{i,t-1}^{es} + \left(\frac{\eta_i^{es,c} P_{i,t}^{es,c}}{C_i^{es}} - \frac{P_{i,t}^{es,d}}{\eta_i^{es,d} C_i^{es}} \right) \Delta t, \tag{10}$$

where $P_{i,t}^{es,c}$ and $P_{i,t}^{es,d}$ are, respectively, the charging and discharging power of energy storage i at time t; $P_i^{es,max}$ is the allowable maximum charging/discharging power; the binary variables $a_{i,t}$ and $b_{i,t}$ equal to 1 when the storage is charging and discharging, respectively, and 0 otherwise; $SOC_{i,min}^{es}$ and $SOC_{i,max}^{es}$ are, respectively, the minimum and maximum allowable SOCs; $\eta_i^{es,c}$ and $\eta_i^{es,d}$ are, respectively, the charging and discharging efficiencies; and C_i^{es} is the rated holding capacity of storage i.

3) *Building*

The building constraints include HVAC heating/cooling power feasible range, heating/cooling complimentary and net power constraints, building thermal dynamics, and indoor temperature comfort [8]. They are expressed below.

$$\begin{aligned} 0 \leq P_{i,t}^{hvac,h} &\leq c_{i,t} P_i^{hvac,max} \\ 0 \leq P_{i,t}^{hvac,c} &\leq d_{i,t} P_i^{hvac,max} \\ c_{i,t} + d_{i,t} &\leq 1 \\ P_{i,t}^{hvac} = P_{i,t}^{hvac,h} &+ P_{i,t}^{hvac,c} \end{aligned} \tag{11}$$

$$\begin{aligned} T_{i,t}^{bldg} &= T_{i,t-1}^{bldg} \\ &+ \psi_{i,in}^{bldg} (\eta_i^{hvac,h} P_{i,t}^{hvac,h} - \eta_i^{hvac,c} P_{i,t}^{hvac,c}) \Delta t \\ &+ \psi_{i,ex}^{bldg} (T_{i,t}^{a} - T_{i,t-1}^{bldg}) \Delta t \\ &+ \zeta_{i,sol}^{bldg} P_{i,t}^{sol} \Delta t \end{aligned} \tag{12}$$

$$T_{i,min}^{bldg} \leq T_{i,t}^{bldg} \leq T_{i,max}^{bldg} \tag{13}$$

Here $\psi_{i,in}^{bldg}$, $\psi_{i,ex}^{bldg}$ and $\zeta_{i,sol}$ are building parameters representing, respectively, the building interior heat capacity, interior-exterior heat exchange capacity and solar irradiation transfer capacity. These building parameters are calculated either from the building physical dimensions and ventilation conditions or from the building heating/cooling historical data. $P_{i,t}^{hvac,h}$ and $P_{i,t}^{hvac,c}$ are, respectively, the heating and cooling power of building i HVAC at time t; $T_{i,t}^{a}$ and $P_{i,t}^{sol}$ are respectively the ambient temperature and solar irradiation; and $T_{i,min}^{bldg}$ and $T_{i,max}^{bldg}$ are, respectively, the minimum and maximum indoor temperature preferences of building i.

4) *EV Charging Station*

The EVSE constraints include its charging power and energy demand bounds, and the EVs' stored energy dynamics as described below.

$$\begin{aligned} P_{i,t}^{evse,min} \leq P_{i,t}^{evse} \leq P_{i,t}^{evse,max} \\ E_{i,t}^{evse,min} \leq E_{i,t}^{evse} \leq E_{i,t}^{evse,max} \end{aligned} \tag{14}$$

$$E_{i,t}^{evse} = E_{i,t-1}^{evse} + P_{i,t}^{evse} \Delta t \tag{15}$$

Bounds $P_{i,t}^{evse,min}$ and $P_{i,t}^{evse,max}$ are, respectively, the aggregate minimum and maximum charging power of EVSEs i at time t; $E_{i,t}^{evse,min}$ and $E_{i,t}^{evse,max}$ are, respectively, the aggregate minimum and maximum energy demands. These EVSE parameters are calculated from charging event data through aggregation of the minimum/maximum charging power and energy demands of the EVs that have arrived at and departed the EVSE. For example, $P_{i,t}^{evse,max}$ is calculated by summing the maximum charging power requirements of all the EVs that are parked for charging (i.e., including arrived but excluding departed EVs at time t) at EVSE i during time t, $E_{i,t}^{evse,min}$ is calculated by cumulatively aggregating the charging energy needed by the EVs that are departed the EVSE at time t and before, and $E_{i,t}^{evse,max}$ is computed by cumulatively adding the energy demanded by the EVs that are arrived at t and before.

5) *Feeder Head (Sub-station) Power*

The feeder head power constraint includes the substation power limit as follows.

$$-P_t^{fh,max} \leq P_t^{fh} \leq P_t^{fh,max} \tag{16}$$

where $P_t^{fh,max}$ is the allowable maximum power exchange between the distribution system and the upstream grid.

6) *Power Balance*

The power balance constraint guarantees the balance between the power generation and demand in the system, and it is given below.

$$\sum_{i \varepsilon D} P_{i,t} + P_{i,t}^{fh} = 0 \tag{17}$$

where D is the set of devices (DERs) in the system, including PVs, storage systems, buildings, EVSEs, and non-controllable loads (L_i).

III. Case Study and Simulation Results

We apply the proposed control approach to two distribution system examples, where each includes 50 and 2,507 controllable devices (DERs), taken from the U.S. bay area synthetic power network [8]. The controllable devices considered in the test systems are curtailable PVs, energy storage systems, and building HVACs and EVSEs. The system parameters used in the study are given in Table I. The formulated control problem is a mixed-integer-linear-program (MILP) and solved by leveraging the XpressMP solver [9]. We first illustrate the simulation results for the test system with 50 devices and then summarize the larger system results later in the section.

TABLE I
SYSTEM PARAMETERS

Parameter	Unit	Value
N		50, 2507
T	Hour	24
Δt	Minute	5, 10, 15, 30, 60, 120
α, β	$\$$/kWh	0.2
δ, γ	$\$$/kWh	0.01
μ	$\$$/kWh	0.0
C_i^{es}	kWh	$2L_i$
$P_i^{es,max}$	kW	L_i
$SOC^{es,min}, SOC^{es,max}$	%	20, 100
$SOC^{es,initial}$	%	90
$\eta^{es,c}, \eta^{es,d}$	%	95, 90
$P_i^{hvac,max}$	kW	$0.1L_i$
$\eta^{hvac,h}, \eta^{hvac,c}$		3
$T_i^{bldg,min}, T_i^{bldg,max}$	°C	20, 23
$T_i^{bldg,initial}$	°C	21
$E_i^{evse,initial}$	kWh	0.0
$P^{fh,max}$	kW	$2\sum L_{i,max}$

Figure 2 shows the aggregate dispatch of each device type versus the locational marginal price (LMP) at the feeder head. The LMP data is taken from the California ISO (CAISO) [10] on a specific day.

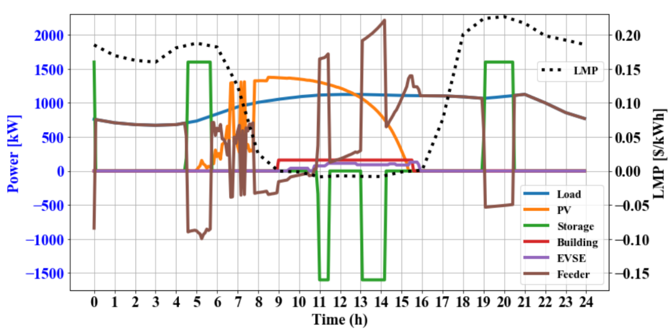

Fig. 2. Aggregate dispatch.

As shown in Fig. 2, during the first 6 hours of operation [0, 6], where the electricity price is high, the energy storage systems discharge, the buildings don't consume power, and the distribution system aggregator not only supplies its local demand but also sold power to the market. During the period [9, 15] where the power price is significantly lower, the distribution system aggregator buys power from the market to supply the local demands, charge the storage systems and preheat the buildings. Of course, the solar power is also higher during this period and supplies the distribution system together with the sub-station (market) power. During the period [19, 21] where the LMP is very high, the storage systems discharge, the distribution system as a whole sells power, and the buildings do not consume power as they are preheated during the previous low-price periods.

Figures 3 and 4 show the scheduling decisions for example single devices. Figure 3 shows scheduling decisions for an EVSE, while Fig. 4 shows the HVAC dispatch for a building.

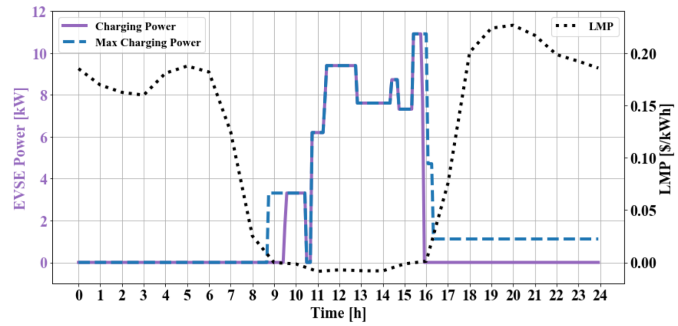

Fig. 3. An EVSE dispatch.

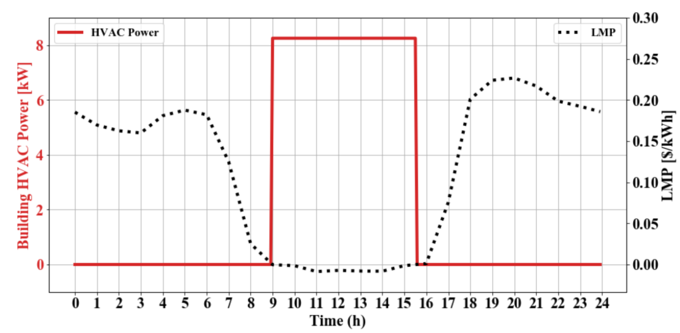

Fig. 4. A building HVAC dispatch.

As shown in Figs. 3 and 4, each device's power dispatch follows the LMP signal where the device dispatches when the market power price is low and/or the renewable power is surplus. This further validates the efficacy of the processed approach in controlling the DERs in the distribution system to meet local load demands and at the same responding to upstream transmission grid (market) signals.

A. Comparison With Simple MPC Formulations

The performance of the proposed variable time granularity with a 24-hour look-ahead horizon MPC (MPC1) is compared against two other MPC benchmarks defined below:

- MPC2: MPC with uniform 5-minute time granularity and 24-hour look-ahead horizon
- MPC3: MPC with uniform 5-minute time granularity and 3-hour look-ahead horizon

MPC2 is a similar problem as MPC1, except it uses the 5-minute time granularity throughout the look-ahead horizon. The optimization problems MPC3 uses are nearly the same size as MPC1 (36 versus 34 time periods, respectively), but with only a 3-hour look-ahead.

The comparison is performed using two metrics, total operating cost and mean computation time (per single run of the MPC), and it is given in Table II. As presented in Table II, the proposed MPC (MPC1) has achieved significant improvement over the benchmark MPC2 with respective to the computation time–a factor of 5.5–with a minor (<0.1%) compromise on the operating cost. MPC3 is more than 2% more expensive than MPC1 or MPC2, while achieving the best computational time.

TABLE II
PERFORMANCE COMPARISON - DISTRIBUTION SYSTEM WITH 50 CONTROLLABLE DERS

Controller	Performance Metric	
	Total Operating Cost ($)	Mean Computation Time (*sec*)
MPC1	420.5627	0.9856
MPC2	420.2215	5.4049
MPC3	430.2215	0.6272

Finally, we investigated the performance of the proposed controller (MPC1) for the larger distribution system containing 2,507 devices. Table III presents the performance comparison of MPC1 with the benchmark controller MPC3 for the larger test system. Preliminary testing showed the MPC2 controller is untenable here, requiring a full 29 minutes ($\gg$ 5 minutes) to complete the first (of 288) control steps. These decisions are no longer relevant, as the control period has long passed. To save computational resources, we did not compute its total operating cost.

TABLE III
PERFORMANCE COMPARISON - DISTRIBUTION SYSTEM WITH 2,507 CONTROLLABLE DERS

Controller	Performance Metric	
	Total Operating Cost ($)	Mean Computation Time (*min*)
MPC1	-567.4760	3.4918
MPC3	-488.3263	2.4464

The performance of the proposed MPC is considerably noticed when we apply the methods on a large-scale distribution grid containing more devices. As given in Table III, MPC1 is able to solve the large system optimal control problem within a few minutes (3.5 minutes), which is sufficiently lower than the duration of the control step (5 minutes). This validates the scalability of the proposed MPC to control massive DERs integrated in large-scale distribution systems where tradition optimal control formulations fail to. The total operating cost values shown in Table III are negative, meaning that the larger system is making a profit by selling the excess power from the solar generation and through energy storage arbitrage and shifting the building and EVSE loads based on the LMP signal.

In summary, observing Tables II and III, the operating cost obtained by the the other benchmark controller MPC3 is higher than the others although it is the fastest. This is because MPC3 has limited capability to look ahead at the future operating conditions of the system and cannot steer the DERs based on future conditions, which is why its total operating cost has increased–costing a full 14% difference in operating costs for the large system. This further confirms the importance of designing controllers with appropriate look-ahead horizons to accurately represent the operation of DERs with inter-temporal constraints (e.g., storage, building, and EVSE) and periodic variations (e.g., PV).

IV. CONCLUSIONS

We solved a look-ahead distribution system power balancing and energy trading problem using a model predictive control approach based on variable time granularity formulation. The proposed controller is applied to distribution systems with different sizes and number of devices. We demonstrated the efficacy of the proposed controller in optimally managing a large number of devices for local power balancing and energy trading profit maximization in a reasonably short computing time. The experimental findings obtained validate the scalability of the controller in controlling thousands of controllable devices in a large-scale distribution system operated via an aggregator. Moreover, the proposed method outperformed other two benchmark controllers regarding computing time and operating cost. Our current findings will continue in the next phase of our research where we will explore the value of the proposed look-ahead controller to guide online decisions considering more distribution network characteristics.

REFERENCES

[1] B. Kroposki et al., "Autonomous Energy Grids: Controlling the Future Grid with Large Amounts of Distributed Energy Resources," in IEEE Power and Energy Magazine, vol. 18, no. 6, pp. 37-46, Nov.-Dec. 2020, doi: 10.1109/MPE.2020.3014540.

[2] E. Dall'Anese and A. Simonetto, "Optimal Power Flow Pursuit," IEEE Trans. on Smart Grid, vol. 9, no. 2, March 2018.

[3] E. Dall'Anese, S.S. Guggilam, A. Simonetto, Y.C. Chen, and S.V. Dhople, "Optimal Regulation of Virtual Power Plants," IEEE Trans. on Smart Grid, vol. 33, no. 2, March 2018.

[4] X.Zhou, Z. Liu, C. Zhao, and L. Chen, "Accelerated Voltage Regulation in Multi-Phase Distribution Networks Based on Hierarchical Distributed Algorithm," IEEE Trans. ob Power Sys., vol. 35, iss. 3, pp. 2047-2058, May 2020.

[5] H. Sheng, C. Wang, B. Li, J, Liang, M. Yang, and Y. Dong, "Multi-timescale Active Distribution Network Scheduling Considering Demand Response and User Comprehensive Satisfaction," IEEE Trans. on Ind. Apps., vol. 67, no. 3, May 2021.

[6] W. Liu and F. Ding, "Collaborative Distribution System Restoration Planning and Real-Time Dispatch Considering Behind-the-Meter DERs," IEEE Trans on Power Sys. vol. 36, no. 4, July 2021.

[7] A.T. Eseye, B. Knueven, X. Zhang, M. Reynolds, and W. Jones, "Resilient Operation of Power Distribution Systems Using MPC-based Critical Service Restoration," in 2021 IEEE GreenTech, April 2021.

[8] W. Liu and F. Ding, "Hierarchical Distribution System Adaptive Restoration With Diverse Distributed Energy Resources," IEEE Trans. on Sust. Energy, vol. 12, no. 2, April 2021.

[9] Q. Chai , C. Zhang and Z.Y Dong, "PV Inverter Reliability-Constrained Volt/Var Control of Distribution Networks," IEEE Trans. on Sust. Energy, vol. 12, no. 3, July 2021.

[10] SMART-DS: Synthetic Models for Advanced, Realistic Testing: Distribution Systems and Scenarios. Available at: https://www.nrel.gov/grid/smart-ds.html

[11] XPRESS. Available at: https://www.fico.com/en/products/fico-xpress-solver

[12] CAISO. Available at: http://www.caiso.com/TodaysOutlook/Pages/prices.html